

Nanoscale

Accepted Manuscript



This is an *Accepted Manuscript*, which has been through the Royal Society of Chemistry peer review process and has been accepted for publication.

Accepted Manuscripts are published online shortly after acceptance, before technical editing, formatting and proof reading. Using this free service, authors can make their results available to the community, in citable form, before we publish the edited article. We will replace this *Accepted Manuscript* with the edited and formatted *Advance Article* as soon as it is available.

You can find more information about *Accepted Manuscripts* in the [Information for Authors](#).

Please note that technical editing may introduce minor changes to the text and/or graphics, which may alter content. The journal's standard [Terms & Conditions](#) and the [Ethical guidelines](#) still apply. In no event shall the Royal Society of Chemistry be held responsible for any errors or omissions in this *Accepted Manuscript* or any consequences arising from the use of any information it contains.

COMMUNICATION

LL37 peptide@silver nanoparticles: Combining the best of the two worlds for skin infection control

Cite this: DOI: 10.1039/x0xx00000x

Mariana Vignoni,^{a,#} Hasitha de Alwis Weerasekera,^a Madeline J. Simpson,^a Jaywant Phopase,^b Thien-Fah Mah,^c May Griffith,^{*b} Emilio I. Alarcon^{*a} and Juan C. Scaiano^{*a,b}

Received 00th January 2012,

Accepted 00th January 2012

DOI: 10.1039/x0xx00000x

www.rsc.org/

Capping silver nanoparticles with LL37 peptide eradicates the antiproliferative effect of silver on primary skin cells, but retains the bactericidal properties of silver nanoparticles with activities comparable to silver nitrate or silver sulfadiazine. In addition, LL37 capped silver nanoparticles have anti-biofilm formation activity.

The human skin is both a physical and immune barrier that protects against colonization by microorganisms. Its many cell types include cells that provide pathogen recognition and defence to production of innate anti-microbial peptides.¹ In burn patients, particularly deeper burns, the barrier integrity is compromised and hence, nosocomial bacterial infections are a major problem in the management of patients in burn care centres.² *Pseudomonas aeruginosa* (*P. aeruginosa*), a Gram negative microbe, in particular, is responsible for much of the recurrent opportunistic bacterial infections, mainly because of biofilm formation.² Other bacteria that contribute to problematic nosocomial infections include Gram positive bacteria, *Staphylococcus epidermidis* (*S. epidermidis*) and *aureus* (*S. aureus*), and Gram negative, *Escherichia coli* (*E. coli*).²

The keratinocytes of the healthy skin produce innate antimicrobial peptides such as the cathelicidin LL37 and defensins.¹ The LL37 peptide displays antimicrobial activity and has a direct effect in wound healing, neovascularization and angiogenesis.³ This peptide has been tested as a potential alternative to antibiotics for treatment of ulcerative wounds and shows good potential.⁴ In the clinic, combinatory use of ionic silver and antibiotics has been proposed as a new strategy to minimize antibiotic resistance.⁵ However, the main shortcoming of using ionic silver, Ag⁺, is that it relies upon the antiproliferative effect that silver has on primary cells.^{2, 6, 7} In burn patients, cell proliferation to repair the wound site is as badly needed as the infection control itself. We have, however, shown that silver nanoparticles (AgNP) that are stabilized with collagen are cell-friendly for primary skin cells and yet demonstrate bactericidal and bacteriostatic effects.⁷ Recent work by Herzog et al., has also

demonstrated the biocompatibility of silver nanoparticles with airway epithelial cells.⁸

In this study, we tested the combination of AgNP with CSG-LL37 peptide, where the -SH served as stabilizer on the AgNP surface^{9, 10} forming LL37@AgNP as a new antimicrobial and anti-biofilm agent. Details of the LL37 synthesis are in SI. Note that the antimicrobial activity, against *P. aeruginosa*, and conformation of LL37 peptide is preserved in truncated peptides containing only the sequence LL7-37 (or RK-31).¹¹

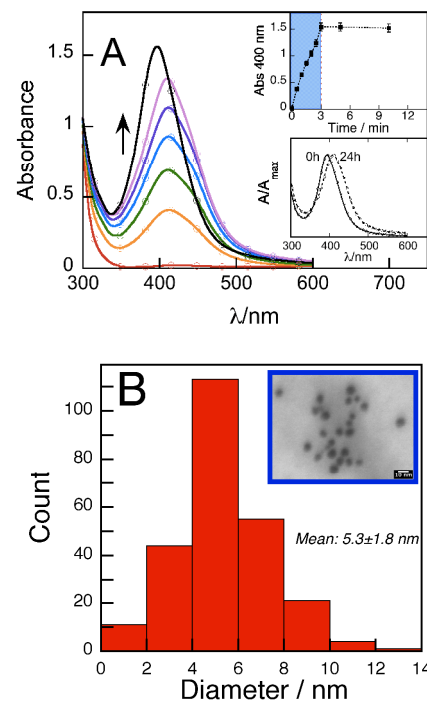
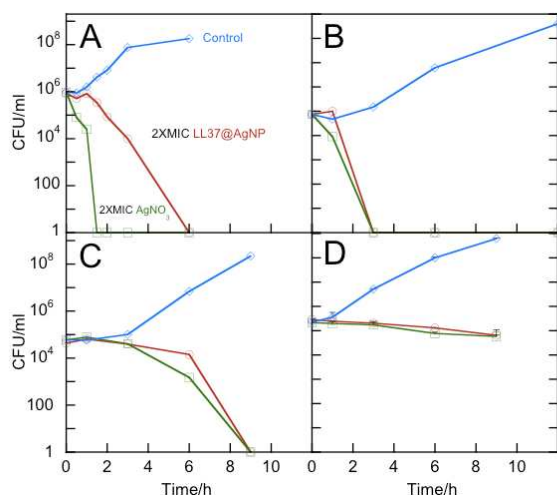


Figure 1. (A) Photochemical formation of LL37@AgNP upon UVA exposure of a oxygen free solution containing 0.2 mM AgNO₃, 0.2 mM L-2959 and 2.5 μM LL37. Absorption spectra taken at different times as indicated in the figure. Top inset: Changes on the absorption at 400 nm vs. irradiation time. Bottom inset:

50 Absorption spectra for LL37@AgNP time 0 after synthesis and 24 h elapsed (B),
 51 Size histogram and TEM image (inset) for a selected area of LL37@AgNP.
 52 Average size calculated from 400 individual particles. The blurriness observed in
 53 the image corresponds to organic material (most likely the LL37 layer around the
 54 particles, see main text) that is being burned during the TEM experiment.

55 The photochemical preparation of biocompatible, protected silver
 56 nanoparticles (AgNP) has been previously reported by our group using
 57 a variety of biomolecules including type I collagen, human serum
 58 albumin, and poly-L-lysine.¹²⁻¹⁴ However, the photochemical synthesis
 59 of peptide capped AgNP remained, however, unexplored. Upon 0.5
 60 min of UVA exposure of oxygen-free aqueous solutions containing
 61 AgNO₃, I-2959 and micromolar concentrations of LL37 peptide, the
 62 formation of an absorption band around 400 nm was observed (Fig.
 63 1A) whose intensity gradually increased up to minute three, where it
 64 reaches a plateau. This is most probably due complete reduction of
 65 Ag⁺ by I-2959 ketyl radical (Fig. S1). The formation of monodisperse
 66 spherical AgNP was observed by both dynamic light scattering (DLS)
 67 and transmission electron microscopy (TEM; Fig. 1B). Note that the
 68 size measured by DLS, 19±1.0 nm, was almost 14 nm larger than the
 69 observed in the TEM, which indicates the formation of a LL37 coating
 70 around the nanoparticle. Zeta potential measurements of
 71 LL37@AgNP revealed a positive potential of +37 ± 0.8 mV, in keeping
 72 with similar zeta potential values previously reported for other
 73 biomolecule capped AgNP.^{12, 13} Only LL37@AgNP were stable up to
 74 24 h in biocompatible buffers or cell culture media, unlike
 75 citrate@AgNP which was unstable (see Fig. S2) or AgNO₃, which
 76 oxidized to silver oxide (data not shown).



77
 78 Figure 2. Number of survival bacteria colonies counted in the presence of 2X MIC
 79 see Table 1 and main text, for AgNO₃ (□) and LL37@AgNP (○) for (A) *E. coli*, (B) *P.*
 80 *aeruginosa*, (C) *S. epidermidis*, and (D) *S. aureus*. Control experiments where no
 81 silver was added are also included (◇). All experiments were carried out in 25%
 82 LB and colonies counted after 18h of incubation at 37°C on agar plates.

83
 84 Table 1 shows that the minimal inhibitory concentration (MIC) for
 85 LL37@AgNP is similar to the control nanoparticles; citrate capped
 86 AgNP (citrate@AgNP), for Gram (-) *P. aeruginosa* and *E. coli*. This is
 87 double the MIC for silver nitrate (AgNO₃) and silver sulfadiazine
 88 (AgSD). For Gram (+) *S. epidermidis* and *S. aureus*, however, the MIC
 89 was similar to AgNO₃ and AgSD. In time kill experiments (Fig. 2),

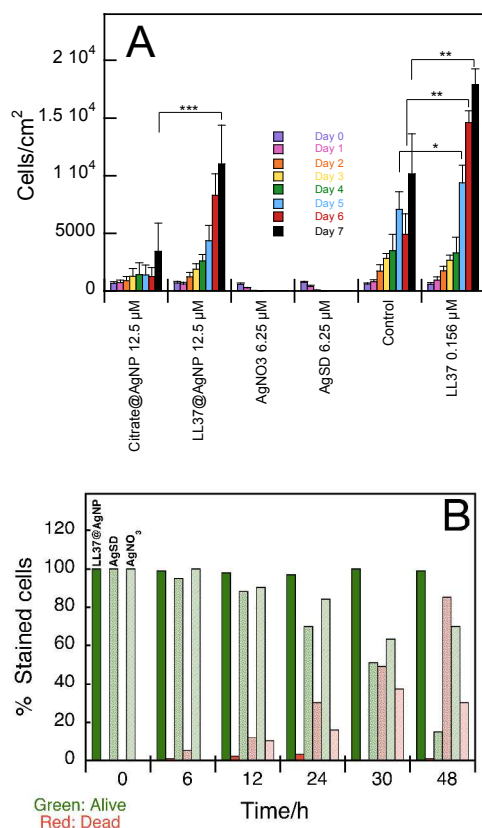
coli was considerably more susceptible to ionic silver, as previously
 reported in literature.²⁵ However, Fig. 2B-D show that the bactericidal
 performance of LL37@AgNP was similar to that observed for AgNO₃
 against *P. aeruginosa*, *S. epidermidis* and *S. aureus*. No bactericidal
 effect of LL37 was observed for all the strains at similar concentrations
 (<0.156 μM) to those in LL37@AgNP (see Fig. S3). All the anti-
 bacterial effects observed appeared to be conferred by AgNP.

Table 1. MIC values in μM for total silver content measured in 25% LB at
 initial bacteria density of ≈ 1x10⁵ cfu/ml.

	<i>E. coli</i>	<i>P. aer.</i>	<i>S. epi.</i>	<i>S. aur.</i>
LL37@AgNP	6.25	6.25	3.12	3.12
Citrate@AgNP	6.25	6.25	6.25	6.25
AgNO ₃	3.12	3.12	3.12	3.12
AgSD	3.12	3.12	3.12	3.12

As mentioned before, delayed wound healing is the main shortcoming
 of using ionic silver in infection prophylaxis.^{2, 6, 7} We have previously
 shown that AgNP were more cell compatible than AgNO₃.^{12, 13} Here,
 we show that our LL37 capped AgNP are not cytotoxic at the MIC or
 even at double the MIC, in contrast to the ionic silver (Fig. S4). In
 addition, LL37@AgNP did not hinder cell proliferation at double the
 MIC, unlike ionic silver, which showed inhibitory effects at half the
 concentration (Fig. 3A). Fig. S4 shows the cell viability measured after
 14 h of incubation in the presence of different silver sources at 2X MIC
 for the opportunistic *P. aeruginosa* where they displayed bactericidal
 properties, see Fig. 2B. At such concentrations, it can be seen that
 AgNO₃ and AgSD have between 60-40% of toxicity, under our
 experimental conditions, with a negligible toxicity for either
 LL37@AgNP or citrate@AgNP (control nanoparticles), see Fig. S4
 (*p*>0.5). Further, cell proliferation experiments up to seven days where
 the silver sources and the cell culture media were replaced every 48 h,
 to somehow mimic sequential topical applications, showed that both
 ionic silver sources delayed the cell proliferation with a total toxicity
 after only day 3, as seen in Fig. 3A. A delay in cell proliferation was
 also observed for citrate@AgNP from day 5 onwards (*p*<0.01) when
 compared to the control. However, with LL37@AgNP, there was no
 significant difference (*p*>0.5) in cell proliferation from the controls
 without any added silver. Note that the cell proliferation values
 measured for citrate@AgNP were considerably smaller than the
 measured at the same total silver concentration of LL37@AgNP, see
 Fig. 3A. These differences become much more important at 1X MIC of
 LL37@AgNP, see Fig. S5, where an increment in the cell proliferation
 from up to day 5 (*p*<0.01) when compared to the control, was
 observed. In this study, the presence of LL37 promoted skin fibroblast
 proliferation by almost a factor of two after seven days (*p*>0.5).
 Control experiments carried out for the ionic silver sources in the
 presence of LL37 show similar trends than those obtained when the
 peptide was not present (see Fig. S6). It has been reported that LL37
 induces proliferation of some epithelial cells, including skin¹⁶ and
 airway epithelial cells.¹⁷ In this study, the stimulatory effect on skin
 fibroblast proliferation appears to be tempered when the peptide was
 conjugated to AgNP (Fig. 3A). Moreover, the antiproliferative effect of
 citrate@AgNP on skin fibroblasts shown in Fig. 3A, was observed only

139 after continued exposure (> 3 days). This behavior points that the
 140 accumulation of toxic products, like AgO,¹³ due to lack of stability of
 141 citrate@AgNP nanoparticles in the cell culture medium, see Fig. S2, is
 142 directly involved in the antiproliferative performance of
 143 citrate@AgNP. Further experiments carried out using Live/Dead
 144 staining for up to 48h in 6h intervals, see Fig. 3B, shown that cell
 145 toxicity is observed within the first 24h of incubation for AgNO₃ and
 146 AgSD, with minimal toxicity for LL37@AgNP or citrate@AgNP (data
 147 not shown). Flow cytometry experiments using Alexa Fluor®488
 148 Annexin and propidium iodide were also carried to detect signs of
 149 early apoptosis and necrosis, respectively.¹⁸ The results presented in
 150 Table 2, see Fig. S7 for representative examples, show that the
 151 samples incubated with AgNO₃ and AgSD for 12h present a
 152 considerably higher necrotic population than either the control or
 153 those containing LL37@AgNP or citrate@AgNP which agrees with
 154 the observed in Live/Dead experiments, see Fig. 3B.



157

158

159 Figure 3. (A) Effect of silver nanoparticles or ionic silver on the proliferation
 160 profile of human skin fibroblasts. Silver source was changed every 48 h in fresh
 161 cell culture media. Error bars correspond to SD from six different samples
 162 obtained from triplicate experiments. T-Student two tail test, *p<0.1, **p<0.01,
 163 ***p<0.001. (B) Percentage of cells stained with AM-Calcein (green bars) or
 164 ethidium bromide homodimer (red bars) measured at different incubation times
 165 after the addition of 12.5 µM LL37@AgNP or 6.25 µM AgSD/AgNO₃. Fluorescence
 166 emission was measured with a FTIC or long pass red filter, for green and red
 167 fluorescence respectively.

168 LL37@AgNP are distinctly more biocompatible than citrate@AgNP
 169 (Fig. 3A) and are more stable (Fig. S2). In addition, the citrate@AgNP
 170 had a tendency to form a black precipitate, most likely AgO when

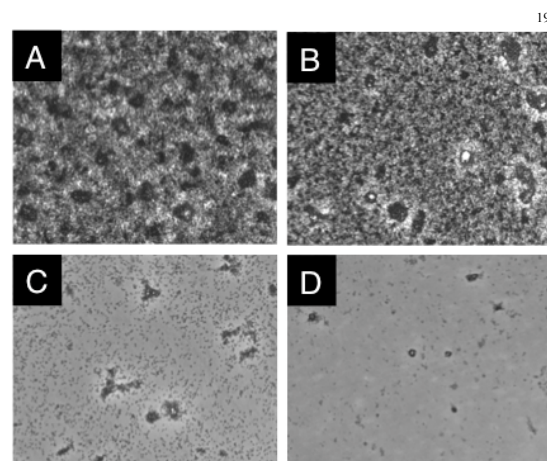
prepared as a thin film at air-liquid interface.¹³ This does not occur
 with LL37@AgNP. Thus, we also tested the capacity of LL37@AgNP
 to prevent the formation of *P. aeruginosa* biofilms using the liquid air
 interface (LAI) assay.¹⁹ The results shown in Fig. 4 indicate that
 LL37@AgNP was able to prevent the formation of the *Pseudomonas*
 biofilm formation at both 1 and 2X MIC concentrations. In contrast,
 LL37 alone was not able to prevent biofilm formation even at twice
 the concentration present in 2X MIC, see Fig. 4. Although further
 testing of the material is still needed prior any clinical application, our
 cumulative data show that the side effects that silver application
 causes in the healing of skin wounds could be solved with the use of
 LL37 capped silver nanoparticles: LL37@AgNP, which provide the
 best of the two worlds; antibacterial properties against Gram positive
 and negative bacteria, and no anti-proliferative effect on primary skin
 cells.

186

187 Table 2. Percentage† of survival, apoptotic and necrotic human skin
 188 fibroblasts cells evaluated using Alexa Fluor®488 Annexin and propidium
 189 iodide (see experimental) after 12h of incubation with the different silver
 190 sources concentrations used in Fig. 3A. In all cases cell densities were kept in
 191 the same range than those employed in all the other cell viability
 192 experiments.

Sample	% Viable cells	% Apoptotic	% Necrotic
Control††	95	1.0	4.0
LL37@AgNP	92	2.0	6.0
Citrate@AgNP	91	4.0	5.0
AgSD	76	6.0	18
AgNO ₃	84	4.0	12

193 †Percentages were calculated in Beckman-Coulter FC500 integrated software
 194 from the Propidium Iodide vs. Alexa Fluore 488 annexin plots. ††Control
 195 experiments were carried out by incubating the cells under the same
 196 conditions that the plates containing the silver sources in DMEM, 10% FBS
 197 with no antibiotics.



198
 Figure 4. Bright field images showing A) *P. aeruginosa* biofilm that had formed
 on the surface of 6 well plates after 16h incubation at 37°C without any anti-
 microbials (control); and B) biofilm formed in the presence of 0.156 µM LL37
 peptide. In the presence of the minimal inhibitory concentration of LL37 coated
 AgNPs (LL37@AgNP), biofilm formation is dramatically reduced (C). At 2 X MIC
 LL37@AgNP, biofilm formation is minimal (D).

206 **Conclusions**

207 The anti-proliferative or toxic effects of ionic silver and silver
208 nanoparticles can be mitigated by the use of silver in form of peptide-
209 stabilized nanoparticles. LL37 did not enhance the anti-microbial
210 effect of the AgNP. Instead, the peptide had a stimulatory on the skin
211 cells. As a composite, LL37@AgNP showed similar anti-microbial
212 activity to clinically used ionic silver, but without the inhibitory effects
213 on cell proliferation and with anti-biofilm activity, which is desirable in
214 promoting wound healing while preventing potential infection in burn
215 care.

216 **Acknowledgements**

217 We thank Dr. Klas Udekwi, Karolinska Institute for the bacterial
218 strains. Support for this work is from a Collaborative Health Research
219 Project grant (NSERC/CIHR Canada) to JCS, NSERC's CREATE
220 program and Swedish Research Council grants to MG and JS.

222 **Notes and references**

223 ^a Department of Chemistry and Centre for Catalysis Research and
224 Innovation, University of Ottawa, Ottawa, Ontario, K1N 6N5
225 ^b Integrative Regenerative Medicine Centre, Departments of Clinical and
226 Experimental Medicine and Physics, Chemistry and Biology, Linköping
227 University, S-58185 Linköping, Sweden
228 ^c Department of Biochemistry, Microbiology and Immunology
229 Faculty of Medicine, University of Ottawa, Ottawa, Ontario, K1H 8M5
230 [#] On leave from: Dep. de Química, Facultad de Ciencias. Exactas, Instituto
231 de Investigaciones Físicoquímicas Teóricas y Aplicadas, Universidad
232 Nacional de La Plata, CCT La Plata-CONICET, La Plata, Argentina
233 *Corresponding author: scaiano@photo.chem.uottawa.ca;
234 emilio@photo.chem.uottawa.ca; mav.griffith@liu.se

235 Electronic Supplementary Information (ESI) available: [Changes on
236 AgNP-SPB absorption; Changes on AgNP-SPB as A/A0 measured in LB
237 or DMEM media; Number of survival colonies in the presence of LL37;
238 Human skin fibroblasts cell toxicity in the presence of different silver
239 sources measured using MTS assay; Effect of LL37@AgNP on the
240 proliferation profile of human skin fibroblasts; Effect of AgSD and
241 AgNO₃ on the proliferation profile of human skin fibroblasts in the
242 presence of LL37 peptide; Representative flow cytometry profiles for
243 human skin fibroblasts stained with Alexa Fluor®488 annexin V/Dead
244 cell apoptosis kit]. See DOI: 10.1039/c000000x/
245
246
247
248

- 249 1. W. R. Heath and F. R. Carbone, *Nat. Immunol.*, **14**, 978-985.
- 250 2. D. Church, S. Elsayed, O. Reid, B. Winston and R. Lindsay, *Clin.*
251 *Microbiol. Rev.*, 2006, **19**, 403-434.
- 252 3. L. Steintraesser, T. Koehler, F. Jacobsen, A. Daigeler, O. Goertz, S.
253 Langer, M. Kesting, H. Steinau, E. Eriksson and T. Hirsch,
254 *Mol. Med.*, 2008, **14**, 528-537.
- 255 4. A. J. Duplantier and M. L. van Hoek, *Front. Immunol.*, 2013, **4**, 1-14.
- 256 5. G. Humphreys, G. L. Lee, S. L. Percival and A. J. McBain, *J.*
257 *Antimicrob. Chemother.*, 2011, **66**, 2556-2561.
- 258 6. Z. Aziz, S. F. Abu and N. J. Chong, *Burns*, 2012, **38**, 307-318.
- 259 7. H. J. Klasen, *Burns*, 2000, **26**, 131-138.

8. F. Herzog, M. Clift, F. Piccapietra, R. Behra, O. Schmid, A. Petri-
Fink and B. Rothen-Rutishauser, *Part. Fib. Toxicol.*, 2013, **10**,
1-14.
9. R. R. Naik, S. E. Jones, C. J. Murray, J. C. McAuliffe, R. A. Vaia and
M. O. Stone, *Adv. Funct. Mat.*, 2004, **14**, 25-30.
10. L. Clem Gruen, *Biochim. Biophys. Acta B.*, 1975, **386**, 270-274.
11. C. Nagant, B. Pitts, K. Nazmi, M. Vandenbranden, J. G. Bolscher, P.
S. Stewart and J.-P. Dehaye, *Antimicrob. Agents Chemother.*,
2012, **56**, 5698-5708.
12. E. I. Alarcon, C. J. Bueno-Alejo, C. W. Noel, K. G. Stampelcoskie,
N. L. Pacioni, H. Poblete and J. C. Scaiano, *J. Nanopart. Res.*,
2013, **15**, 1374-1377.
13. E. I. Alarcon, K. Udekwi, M. Skog, N. L. Pacioni, K. G.
Stampelcoskie, M. Gonzalez-Bejar, N. Poliseti, A. Wickham,
A. Richter-Dahlfors, M. Griffith and J. C. Scaiano,
Biomaterials, 2012, **33**, 4947-4956.
14. M. J. Simpson, H. Poblete, M. Griffith, E. I. Alarcon and J. C.
Scaiano, *Photochem. Photobiol.*, 2013, **89**, 1433-1441.
15. Q. L. Feng, J. Wu, G. Q. Chen, F. Z. Cui, T. N. Kim and J. O. Kim, *J.*
Biomed. Mater. Res., 2000, **52**, 662-668.
16. J. D. Heilborn, M. F. Nilsson, G. Kratz, G. Weber, O. Sorensen, N.
Borregaard and M. Stahle-Backdahl, *J. Investig. Dermatol.*,
2003, **120**, 379-389.
17. R. Shaykhiev, C. Beisswenger, K. Kandler, J. Senske, A. Puchner, T.
Damm, J. Behr and R. Bals, *Am. J. Physiol. Lung Cell. Mol.*
Physiol., 2005, **289**, L842-L848.
18. Z. Darzynkiewicz, G. Juan, X. Li, W. Gorczyca, T. Murakami and F.
Traganos, *Cytometry*, 1997, **27**, 1-20.
19. J. H. Merritt, D. E. Kadouri and G. A. O'Toole, in *Curr. Prot.*
Microbiol., John Wiley & Sons, Inc., 2005.